A high accuracy ultrasonic distance measurement system using binary frequency shift-keyed signal and phase detection

S. S. Huang
Department of Electrical Engineering, National Cheng-Kung University, 70101 Tainan, Taiwan, Republic of China

C. F. Huang
Department of Electrical Engineering, Kao Yuan Institute of Technology, 82101 Kaohsiung, Taiwan, Republic of China

K. N. Huang and M. S. Young[a)]
Department of Electrical Engineering, National Cheng-Kung University, 70101 Tainan, Taiwan, Republic of China

(Received 10 April 2002; accepted for publication 18 June 2002)

A highly accurate binary frequency shift-keyed (BFSK) ultrasonic distance measurement system (UDMS) for use in isothermal air is described. This article presents an efficient algorithm which combines both the time-of-flight (TOF) method and the phase-shift method. The proposed method can obtain larger range measurement than the phase-shift method and also get higher accuracy compared with the TOF method. A single-chip microcomputer-based BFSK signal generator and phase detector was designed to record and compute the TOF, two phase shifts, and the resulting distance, which were then sent to either an LCD to display or a PC to calibrate. Experiments were done in air using BFSK with the frequencies of 40 and 41 kHz. Distance resolution of 0.05% of the wavelength corresponding to the frequency of 40 kHz was obtained. The range accuracy was found to be within ± 0.05 mm at a range of over 6000 mm. The main advantages of this UDMS system are high resolution, low cost, narrow bandwidth requirement, and ease of implementation. © *2002 American Institute of Physics.* [DOI: 10.1063/1.1502017]

I. INTRODUCTION

The techniques of distance measurement using ultrasound in air include the time-of-flight (TOF) technique,[1–3] single-frequency continuous wave phase shift,[4] two-frequency continuous wave method,[5] combining methods of TOF and phase-shift,[6] multifrequency continuous wave phase shifts,[7,8] and a multifrequency AM-based ultrasonic system.[9] The TOF method has been extensively discussed in recent literature. The pulse propagates through the transmission medium and is reflected by a suitable reflector. The time taken for the pulse to propagate from transmitter to receiver is proportional to the reflector's range. The distance between the reflector and transducer site is $d=(c*\mathrm{TOF})/2$, where c is the sound velocity. Using TOF to measure the distance, the system errors are primarily due to amplitude degradation of the received signal, and uncertainty in the speed of sound. The method is more efficient when the energy transferred between emission and reception is high, but it is strongly limited by the ultrasonic transducers, which must be of rather high quality factor, high power, and high cost. Increasing the frequency of the pulse transmitted can improve the accuracy and the resolution, but the higher frequency of the pulse transmitted, the greater the attenuation per unit distance. Therefore the maximum measurable distance will also be reduced. Normally, if distances in air of a few meters are to be measured, frequencies in the range 20–100 kHz must be used in order to maintain suitable receiver signal levels.[10] So the TOF method of range measurement is subject to high levels of errors (about 1 cm) when used in an air medium, thus limiting its applications.

In order to obtain accurate distance estimations, a superior system choice is the phase data of a steady-state frequency received signal with reference to its transmitted signal. This is because the distance information is derived from the phase difference of a repeating signal which is sampled for a statistically significant number of wave periods. Thus, the random variations in phase shift (from turbulence, environmental noise, electronic noise, etc.) tend to cancel themselves out in an averaging process. Most applications of range measurement in air using ultrasound apply a phase-shift analysis of single-frequency continuous-wave transmission.[4,10,11] If the transmitter is energized with a continuous sinusoidal signal, the signal corresponding to the received acoustic wave can be written as $Vr(t)=Ar\sin(\omega t+\theta)$. Here Ar is the peak value of the received signal, ω is the resonant angular frequency of the transducer, and θ is the phase shift, which is linearly proportional to the measured target distance. The range or distance L can be determined by the phase shift θ of a single frequency if the maximum ranging distance does not exceed one full wavelength; otherwise phase ambiguity will occur. Obviously, the maximum achievable range for transducer with a resonant frequency of 40 kHz is about 4.25 mm (corresponding to an ultrasound

a)Author to whom correspondence should be addressed; electronic mail: msyoung@mail.ncku.edu.tw

velocity of 340 m/s) which is usually too short for most ranging applications. Although this disadvantage can be improved by a multiple-frequency continuous wave technique,[7] which calculates the target distance at ranges much greater than one wavelength, the range of measurement is still too short (only 1500 mm).

Gueuning *et al.* present an algorithm for range measurement, which combines both the pulse TOF method and the phase-shift method,[6] and can obtain accurate distance measurement (better than 1 mm). The technique is based on a particular signal processing method which determines the approximate TOF by computing the crosscorrelation between the envelope of the transmitted and received signals. The carrier phase shift between emission and reception is then computed in order to refine the final result. But the accuracy of this computed the phase shift is limited by the amplitude accuracy of the samples and the resolution of the analog to digital (A/D) converter, and the refined range does not exceed a wavelength of the transmitted signals. Webster presents a method that is based upon the binary frequency shift-keyed (BFSK) signal (with two frequencies of $f1$ and $f2$) followed by data acquisition and signal processing of phase-digitized information from the received signal.[10] The method can reduce many of the problems that arise when dealing with the nonideal behavior of ultrasonic transducers. But the TOF is estimated by the time at which the transition between $f1$ and $f2$ occurs and is determined from the phase data, which are easily influenced by noise, and errors arise.

This article also uses combined methods to achieve better, more accurate distance measurement, but the approach adopted in this article is a new one. The new algorithm to measure the distance has two independent parts. One part estimates the TOF, and the other part calculates the phase-shift difference between the transmitted and received signal. The proposed method is based upon the transmission of a BFSK signal.[10] Upon reception of the pulse, the TOF is computed by the time at which the change between each discrete frequency occurs and two phase shifts between the transmission and reception signals are detected in order to enhance the accuracy of the time measurement. The phase shifts are computed by a counter technique to avoid the limitation caused by the amplitude of the signal and the finite bits of the A/D converter. A new algorithm in this article is developed to calculate the target distance, and the proposed range measurement system can obtain accuracy and resolution that is higher than previous methods.[6,7,10]

II. THE MEASUREMENT ALGORITHM

The principle of the ranging system is similar to the operation of using a ruler. At first a coarse measurement is done, and then a fine measurement is adopted to refine the final result. Thus the high accuracy is achieved.

A. Transmitted signals and received signals

The transmitted signals and the received signals are shown in Fig. 1. The S_T is the transmission signal of a BFSK which has two frequencies $f1$ and $f2$ shown in Fig. 1(a). The Tr is the period of S_T. The S_R is the received signals corresponding to the transmitted signals as shown in Fig. 1(b).

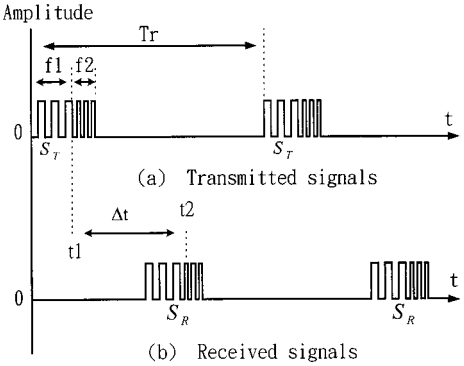

FIG. 1. Transmitted signals and received signals.

B. Signal processing of received signals

There are two steps to processing of the received signal.

1. Calculation of the TOF

The method to calculate the TOF is as follows. In Fig. 1 the elapsed time Δt, which is the round-trip travel time of the transmitted signal from the transmitter to the reflective target and back to the receiver, can be calculated by received/transmitted signals and written as $\Delta t = t2 - t1$. Here $t1$ is the time when $f1$ changes to $f2$ of the transmitted signal, $t2$ is the time when $f1$ changes to $f2$ of the received signals corresponding to the transmitted signals. The ranging distance can be expressed as $d = (c * \Delta t)/2$, where c is the sound velocity.

2. Detection of the phase shift

The detection of the phase shift is based on the two-frequency continuous wave method of ultrasonic distance measurement.[5] The phase shift of $\theta1$ and $\theta2$ can be detected by the received signals corresponding to the transmit signals. A continuous wave with frequency $f1$, and a received signal (S_R) with frequency $f1$ and $f2$ are shown in Fig. 2. The phase shift $\theta1$ is the difference in phase between the continuous wave and the received signal at $f1$. The phase $\theta1$ can be written as $\theta1 = 2\pi(t2 - t1)/T1$, where $T1$ is the period of the received signal of $f1$. Similarly, the phase $\theta2$ is the dif-

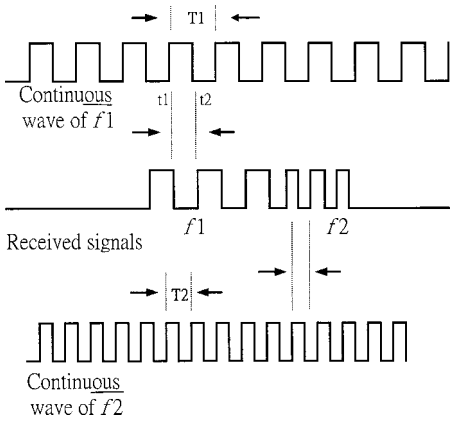

FIG. 2. Illustration of the phase shift $\theta1$, $\theta2$.

ference in phases regarding the received signal at $f2$. Comparison of the two phase shifts allows calculation of target range. The formulas can be written as

$$L=\frac{1}{2}*\left(n1+\frac{\theta 1}{2\pi}\right)*\lambda 1 \tag{1}$$

and

$$L=\frac{1}{2}*\left(n2+\frac{\theta 2}{2\pi}\right)*\lambda 2, \tag{2}$$

where L is the distance between the target and transducer site, $\lambda 1$, $\lambda 2$ are the wavelengths of the ultrasound, $n1$, $n2$ are integers, and $\theta 1$, $\theta 2$ are phase shifts.

Due to the different wavelengths, the expression for the difference of the phase shift may be derived from Eqs. (1) and (2) as follows:

$$\Delta\theta=\pi*L*\left(\frac{1}{\lambda 2}-\frac{1}{\lambda 1}\right). \tag{3}$$

The integers $n1$ and $n2$ in Eqs. (1) and (2) have only two possible values: $n1=n2$ and $n2=n1+1$. So the difference of the phase shifts can be defined by the following algorithm:

(1) If $\theta 2>\theta 1$, then $\Delta\theta=\theta 2-\theta 1$ and
(2) If $\theta 2<\theta 1$, then $\Delta\theta=\theta 2-\theta 1+\pi$.

If the velocity of ultrasound is constant, say c, the wavelength λ can be determined as: $\lambda 1=c/f1$, $\lambda 2=c/f2$. Here, $f1$ and $f2$ are the frequencies of the ultrasonic wave. From Eq. (3), the ranging distance can be expressed as

$$L=\frac{\Delta\theta}{\pi}*\frac{c}{\Delta f}\quad(\Delta f=f2-f1). \tag{4}$$

The ranging distance L can be uniquely determined by the difference of the phase shifts $\Delta\theta$ ($\Delta\theta=\theta 2-\theta 1$), if the maximum ranging distance does not exceed the half of wavelength of Δf. Otherwise a phase ambiguity will occur. The maximum achievable detecting range with Eq. (1) is about 4.375 mm and with Eq. (4) is about 175 mm (taking $c=350$ m/s, $f1=40$ kHz, $f2=41$ kHz).

C. Computation of the distance

The algorithm derived for computing distance d is explained as follows. The ranging distance d can be obtained by $d=(c*\Delta t)/2$, where the Δt is TOF. The range d is divided into regions $[(k-1)Lr,kLr]$ $(k=1,2,3,...)$ in Fig. 3(a). The Lr is the wavelength of Δf. The ranging distance d can be expressed as $d=1/2*[(k-1)+(\Delta\theta/2\pi)]*c/\Delta f$, where k is an integer. The region defined by $[(k-1)Lr,kLr]$ is referred to as the No. k region. The $k-1$ integer can be obtained by $\mathrm{Int}(\Delta t*\Delta f)$, where Int[ ] is the integer operation. So the estimate of target distance can be expressed by the following algorithm:

$$d=\frac{1}{2}*\left[\mathrm{Int}(\Delta t*\Delta f)+\frac{\Delta\theta}{2\pi}\right]*\frac{c}{\Delta f}. \tag{5}$$

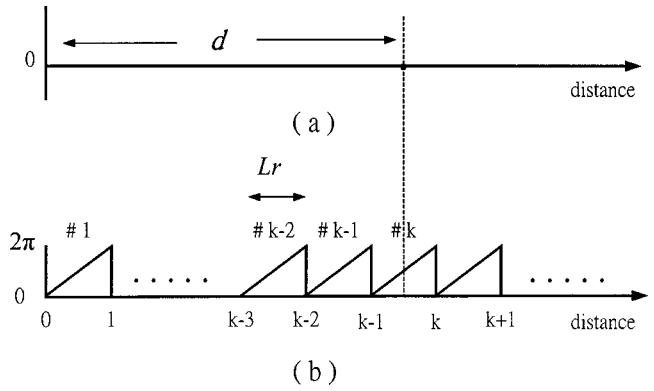

FIG. 3. Relation between $d=c*\Delta t$ and $d=(k-1)*Lr+(\Delta\theta/2\pi)*Lr$.

In order to increase the accuracy, the No. k region can be divided by l, where $l=\lambda 1=c/f1$ in Figs. 4(b) and 4(c), and the fine scale measurement of $(\Delta\theta/2\pi)*(c/\Delta f)$ can be replaced as $(m+\theta 1/2\pi)*c/f1$, where the integer m can be gotten by $\mathrm{Int}[(\Delta\theta/2\pi)*(f1/\Delta f)]$. The final estimate of target distance can be expressed as

$$d=\frac{1}{2}*\mathrm{Int}(\Delta t*\Delta f)*\frac{c}{\Delta f}+\frac{1}{2}*\left[\mathrm{Int}\left(\frac{\Delta\theta}{2\pi}*\frac{f1}{\Delta f}\right)+\frac{\theta 1}{2\pi}\right]*\frac{c}{f1}. \tag{6}$$

The algorithm for d can be easily developed into the digital microprocessor's system to detect target distance with the benefits of high accuracy and low cost.

III. SYSTEM IMPLEMENTATION

A block diagram of the ultrasonic distance measurement system (UDMS) is shown in Fig. 5. This system consists of two acoustic transducers with matching exponential horns, a signal generation system, power amplifier, preamplifier and gain-controlled system, frequencies detected system, digital

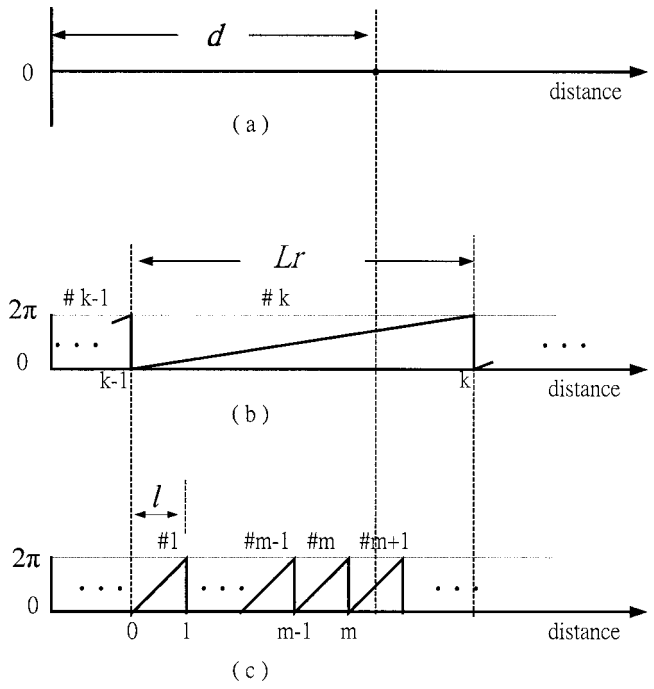

FIG. 4. Relation of d, Lr, and l.

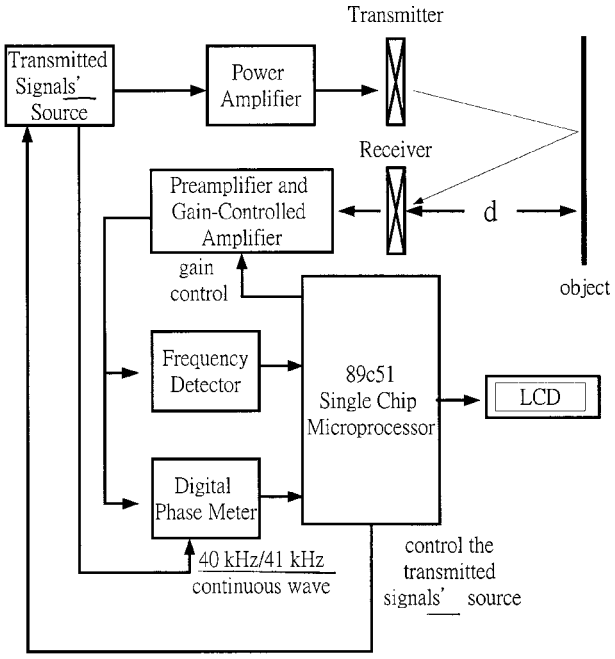

FIG. 5. Block diagram of the UDMS.

phase meter, and calibration system. A microprocessor-based controller governs the operation of the entire system.

A. Hardware of the system

Analysis of the operation of the system can be conveniently divided into six parts. The operation of each module is described as follows.

1. Transmitted signal source

The transmitted pulse is made up of two sinusoids (40 and 41 kHz) of approximately 60 cycles at each frequency. The block diagram of the transmitted signals' generation system is shown in Fig. 6. A crystal oscillator circuit is used to generate a stable signal with a base frequency of 80 MHz. The 50% duty cycle can be obtained by two dividers. The output frequency of the divider No. 1 is 40 kHz and the output of divider No. 2 output is 41 kHz. Both outputs are sent to the multiplexer (MUX). The MUX is controlled by an 89c51 microprocessor. The output of the MUX is a BFSK

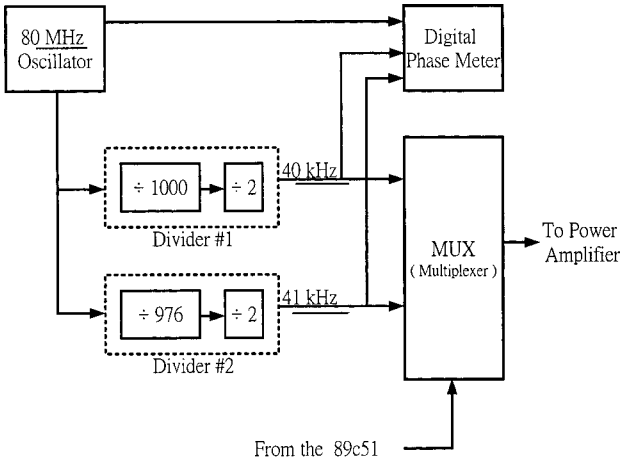

FIG. 6. Block diagram of the transmitted signals' source.

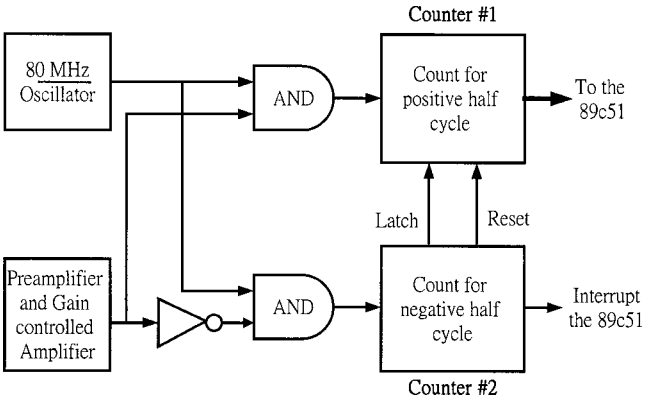

FIG. 7. Block diagram of the frequency detector.

signal which is similar to the transmitted signal shown in Fig. 1(a). The BFSK signal is generated in digital form and delivered to the power amplifier, and then to the transmitting transducer.

2. The preamplifier and the gain-controlled amplifier

The bandwidth of the ultrasonic transducer that we are considering is narrow. To avoid error from acoustic attenuation, the gain of the amplifier must adjust automatically when the frequency of the ultrasound changes. Therefore, the error related to acoustic attenuation is minimized in the gain-controlled amplifier by keeping the received signal amplitude dynamically constant. Another function at this stage is to detect the zero crossing point of the received signal, and to translate it into a TTL compatible square wave whose duty cycle is 50%.

3. Frequency detector

The block diagram of the frequency detector is shown in Fig. 7. The frequency detector detects the time when $f1$ (40 kHz) change to $f2$ (41 kHz) of the received signal. The detected time is then computed by the microprocessor to obtained TOF. Two counters are designed to distinguish the $f1$ or $f2$ frequency. The clock of counter No. 1 is the output of an AND Gate with the input of 80 MHz clock and the TTL compatible square wave received signal. If the counted value of counter No. 1 is about 1000, then the frequency of the received signal is determined as 40 kHz, and the value about 976 corresponds to 41 kHz. Counter No. 2 is used to latch and reset counter No. 1, and interrupt the 89c51 microprocessor.

4. The digital phase meter

The block diagram of the digital phase meter is shown in Fig. 8. The main function of the phase-shift converter (PSC) is to convert the phase shift data into the pulse width with two dividers ($\div 2$) and one XOR gate. The procedure of the PSC can be simply described as follows and shown as in Fig. 9.

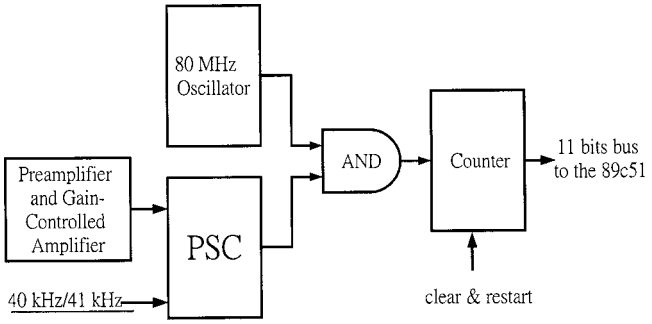

FIG. 8. Block diagram of the digital phase meter.

(a) Step 1: The 40 or 41 kHz signals [shown as Fig. 9(a)] are divided into 20 or 20.5 kHz signals as shown in Fig. 9(b).
(b) Step 2: The received signals [shown as Fig. 9(c)] are divided by 2 as shown in Fig. 9(d).
(c) Step 3: The result of the XOR gate shown in Fig. 9(e) is obtained with the input signals of 20 kHz/20.5 kHz gotten from step 1 and the signals gotten from step 2.

The result obtained from step 3 is the pulse width. A counter (in Fig. 8) based on 80 MHz oscillator is used to count the pulse width. The phase shift θ can be expressed as $\theta = 360^* \varphi_w / \varphi_T$, where φ_w is the counted value of the pulse width by the counter, and φ_T is the counted value of a cycle. The range-equivalent resolution of the phase meter is 0.05% of the wavelength for a 40 kHz. Finally, the counter is cleared by the microprocessor and ready for counting the next phase shift.

5. 89c51 single-chip microprocessor

The UDMS system is governed by an 89c51 single-chip microprocessor. The main function of the microprocessor is to control the BFSK of the ultrasound, get the digital phase shift, evaluate the TOF, calculate the target distance, and display it.

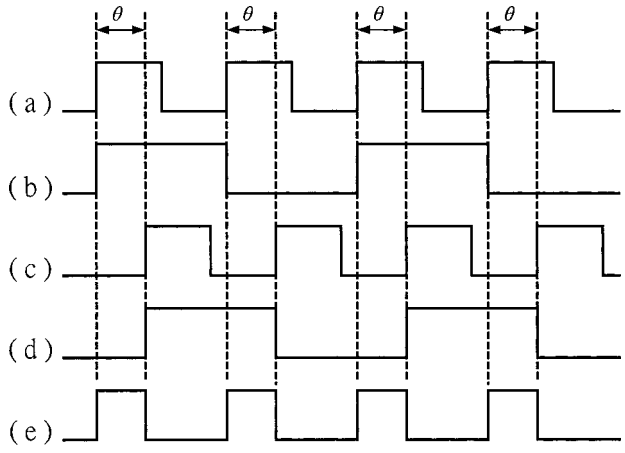

FIG. 9. Charts of the operations of the PSC. (a) 40 kHz/41 kHz signal. (b) 20 kHz/20.5 kHz signal. (c) The received signal. (d) The divided signal of the received signal. (e) The output signal of the XOR gate.

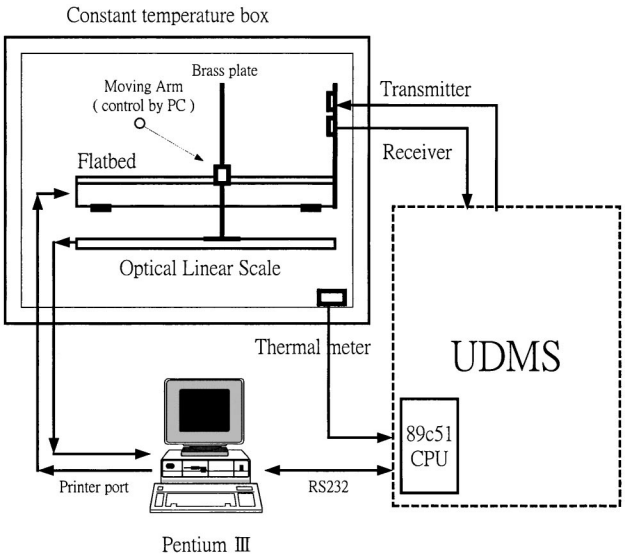

FIG. 10. Block diagram of the calibrating system.

6. Calibration system

The UDMS system must be calibrated with a known distance. The following procedure assumes constant sound speed over the entire range. The experimental embodiment of the distance measurement system is shown in Fig. 10, which consists of a constant temperature box, a brass plate (which is used as a reflector and mounted on a step motor's arm), an optical linear scale, and a Pentium III. The reference scale of an optical linear measuring device (Pulscale model SJH5515AAR, Futaba, Japan) is mounted on the stepping motor. An optical sensor and its reflector are attached to each other and fixed in the stepping motor's arm. The stepping motor's arm changes the position of the reflector. Thus, for any given position, the PC is provided the elapsed time of Δt, phase data, and optically measured distance, allowing the PC to calculate and display the error of distance that can be used for calibration.

B. Software of the system

The software program of the microcomputer is described by the flowchart in Fig. 11. The 89c51 microprocessor will assign the transmitted signal, adjust the gain-controlled amplifier, and wait to be interrupted by the frequency detector or digital phase meter to evaluate the TOF, get $\theta 1$, $\theta 2$, and calculate the distance. The 89c51 will assign the transmitted signal again if the waiting time is more than 50 ms. During the calibration phase, the TOF, $\theta 1$, and $\theta 2$, are sent to the PC via the 89c51's RS232 interface. After calibration, the data of measurement distance is displayed on the LCD.

IV. TESTING THE SYSTEM

A prototype range measurement system was tested in the laboratory by comparing the calculated distance obtained from UDMS and the distance measured by the optical scale. The center frequency of the transmitted/received transducer was 40 kHz and the bandwidth was 2 kHz. The testing device is described in Sec. III A 6. The temperature in the constant temperature box was set to 28 °C. We know the tem-

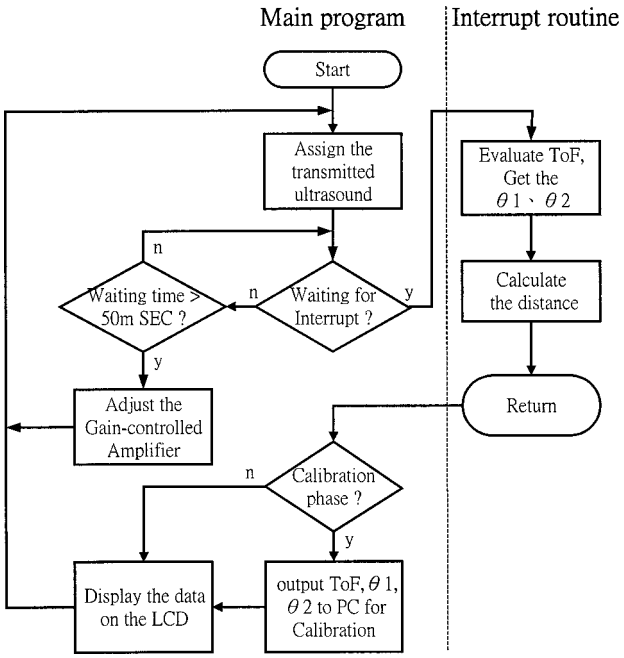

FIG. 11. The flowchart of the software.

perature is $28\pm0.1\,^{\circ}\mathrm{C}$ along the path. The accuracy of the phase shifts were verified by the standard instrument (HP Universal Counter).

There were approximately ten cycles (approximately 250 μS) of the received signal while the frequency was transitionally varied from 40 to 41 kHz as shown in Fig. 12. The frequency of the transition wave was sequentially changed as 40, 40.1, 40.2, 40.3,... to 41 kHz. Owing to this phenomenon, the system had to wait for approximately 250 μS until the frequency of the received signal settled to its steady state value of 41 kHz, and detected the phase shift $\theta 2$. The system also had to decrease the error induced when TOF was estimated. The error can be reduced by the following algorithm.

(a) Step 1: Given a distance L, the estimated elapsed time $t1$, can be written as $t1=\Delta t+t_e$, here Δt was the actual elapsed time, t_e was the error.
(b) Step 2: Given a distance $2L$, the estimated elapsed time $t2$ can be written as $t2=2\Delta t+t_e$.
(c) Step 3: From step 1 and step 2, the t_e can written as $t_e=2t1-t2$.

The final result t_e will be saved and used as calibration data.

V. EXPERIMENTAL RESULTS

A logged data graph of the elapsed time versus distance ranging from approximately 1000 to 6000 mm was shown in Fig. 13(a). The error data in the error plots in Fig. 13(b) were the difference between the theoretical TOF and the measured TOF. The theoretical TOF value was calculated by $\Delta t=L/c$ and $c=\sqrt{RT\gamma/M}$.[12] Here L is distance (meter), c is the speed of sound (m/s), R is the universal gas constant (8314.48 J/kmol K), T is the absolute temperature (in K), γ is the ratio of specific heats ($\gamma=Cp/C\nu=1.4005$), and M is the molar mass (28.95 kg/kmol). The standard errors (SE) of the TOF were calculated by the following equation:

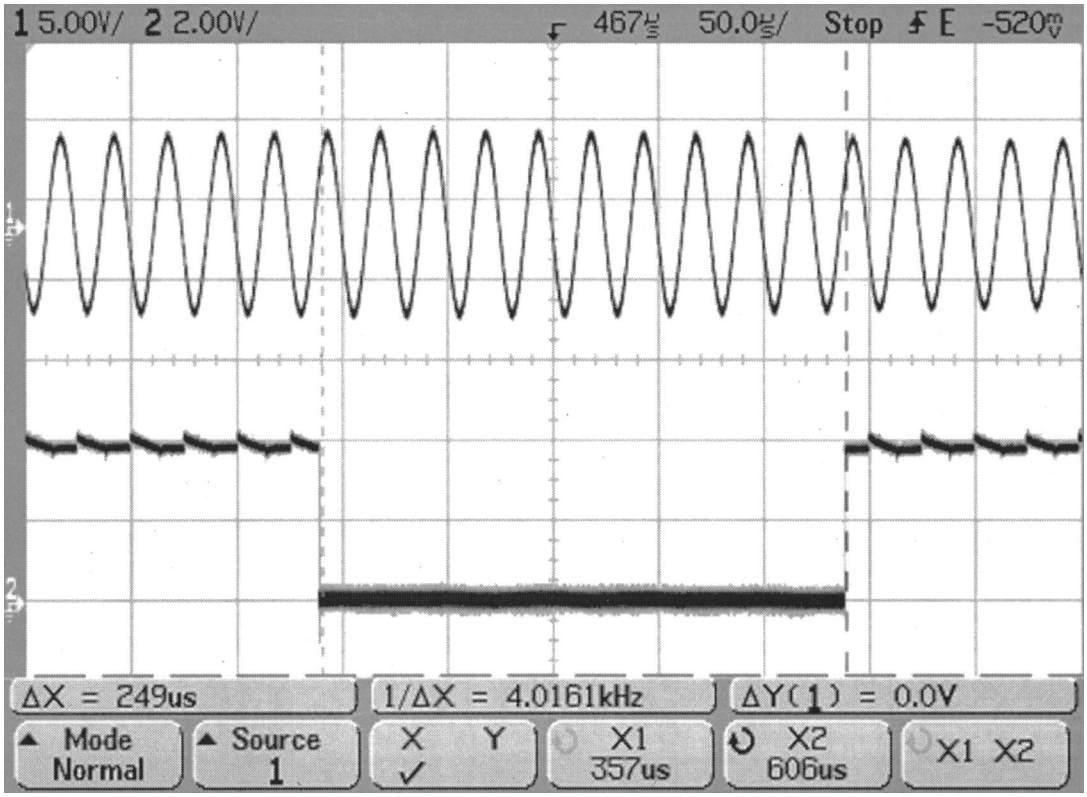

FIG. 12. The frequency of the transition wave was varied from 40, 40.1, 40.2, 40.3,... to 41 kHz.

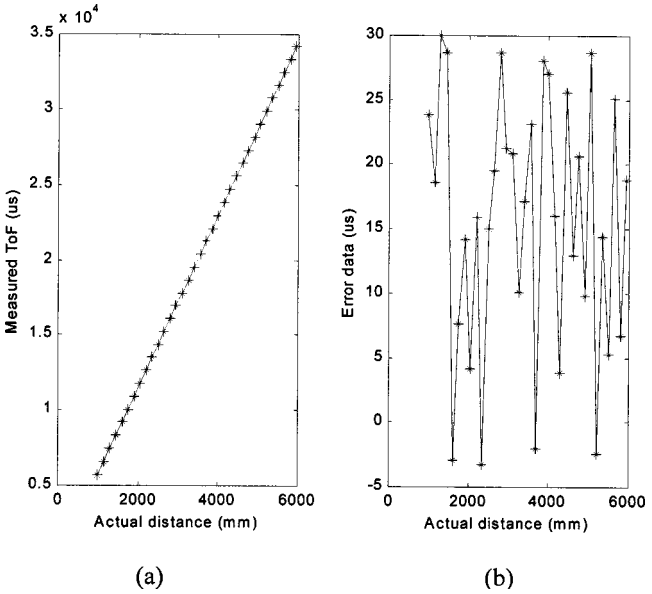

FIG. 13. (a) A logged data graph of the elapsed of time vs distance. (b) The error plot of the TOF.

$$\mathrm{SE}=\sqrt{\sum_{i}^{n}\frac{[RP(i)-PP]^2}{n}}, \tag{7}$$

where *RP* is the TOF measured by the UDMS system, *PP* is the theoretical value of the TOF, and *n* is the number of measured data points. The average error of the TOF was 18.5 μS and then the error in measured distance was 2.87 mm. The error in measured distance by the TOF method could be refined by a phase shift method in the UDMS system.

A logged data graph of the actual distance versus measured distance from approximately 1000 to 6000 mm is shown in Fig. 14(a). The error plot is shown in Fig. 14(b). The standard errors of the measured results were calculated by Eq. (7), where *RP* is the distance calculated by the UDMS, *PP* is the distance measured by the optical scale, and *n* is the number of measured data. The average error was 0.0216 mm. Through the repeated experiments, the average SE was consistently kept within ± 0.05 mm over 6000 mm.

VI. DISCUSSION

A new highly accurate binary frequency shift-keyed UDMS system for use in isothermal air has been presented. This system successfully combines both the TOF method and the phase-shift method. The technique is based on the BFSK transmitted signal. Upon reception of the pulse, the approximate TOF is computed by the time at which the change between each discrete frequency occurs. Two phase shifts

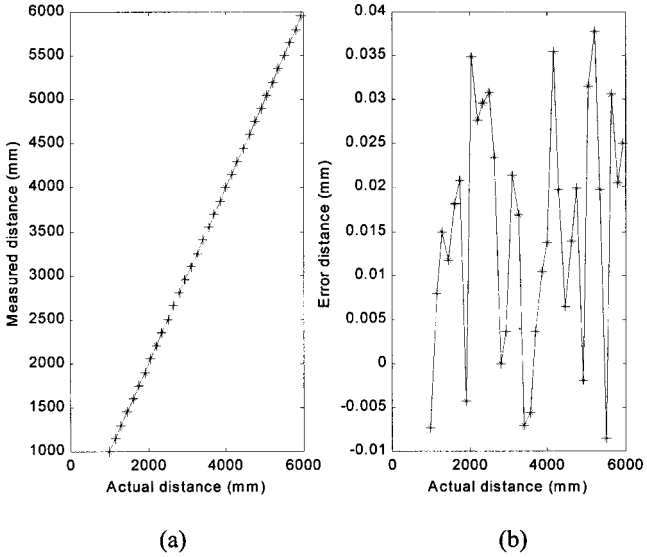

FIG. 14. (a) A logged data graph of the actual distance vs calculated distance. (b) The error plot of distance.

between the transmission and reception signals are computed in order to enhance the accuracy of the result. The phase shifts are computed by a counter technique to avoid the limitation caused by the amplitude of the signal and the finite bits of the A/D converter.

The phase shifts will be influenced by the speed of sound. If the measured distance is within 6 m, and the errors of measured phase shift vary within one degree, the velocity error of sound can be kept within ± 0.003 m/s. A resolution of 0.05% of the wavelength corresponding to the frequency of 40 kHz was obtained and the range accuracy was found to be within ± 0.05 mm over 6000 mm.

[1] D. Marioli, IEEE Trans. Instrum. Meas. **41**, 93 (1992).
[2] M. Parrilla, J. J. Anaya, and C. Fritsch, IEEE Trans. Instrum. Meas. **40**, 759 (1991).
[3] G. Tardajos, G. G. Gaitano, and F. R. M. de Espinosa, Rev. Sci. Instrum. **65**, 2933 (1994).
[4] M. S. Young and Y. C. Li, Rev. Sci. Instrum. **63**, 5435 (1992).
[5] J. S. Shoenwald and C. V. Smith, Jr., Proceedings of the IEEE Ultrasonic Symposium, 1984, p. 469 (unpublished).
[6] F. E. Gueuning, M. Varlan, C. E. Eugene, and P. Dupuis, IEEE Trans. Instrum. Meas. **46**, 1236 (1997).
[7] C. F. Huang, M. S. Young, and Y. C. Li, Rev. Sci. Instrum. **70**, 1452 (1999).
[8] T. Kimura, S. Wadaka, K. Misu, T. Nagatsuka, T. Tajime, and M. Koike, IEEE Ultrasonic Symposium, 1995, p. 737.
[9] M. Yang, S. L. Hill, and J. O. Gray, IEEE Trans. Instrum. Meas. **43**, 861 (1994).
[10] D. Webster, IEEE Trans. Instrum. Meas. **43**, 578 (1994).
[11] F. Figueroa and E. Barbieri, IEEE Trans. Instrum. Meas. **40**, 764 (1991).
[12] G. S. K. Wong and T. F. W. Embleton, J. Acoust. Soc. Am. **77**, 1710 (1985).